

SIMULATION OF MELTING OF ALLOYING MATERIALS IN STEEL LADLE

Petri Väyrynen, Lauri Holappa, and Seppo Louhenkilpi

Aalto University, School of Chemical Technology, Department of Materials Science and Engineering, PO Box 16200, FI-00076, Espoo, Finland

Abstract

Additions to the liquid steel in ladle are performed to attain the desired steel composition and to purify the steel to improve its cleanliness. The added materials differ regarding to size, shape, density, melting point, latent heat of fusion etc. Further the liquid steel composition, temperature and flow conditions influence the phenomena in heating, melting and dissolution of the added object. Solidification of steel shell around the added object is an initial event in lump additions too. In this study different phenomena were modeled for different materials by using commercial Flow-3D CFD software. Simulation of the shell formation procedure was divided into two stages. In the first stage a cold alloy lump is introduced into the liquid steel and solid shell starts to form, it grows to a maximum thickness and then starts to melt and finally disappears. In the second stage the lump itself melts, if not yet molten, and is mixed into the bulk steel in the ladle. Simulations were done for aluminium, FeSi, FeMn, SiMn and FeCr with selected lump sizes. Solid shell development and existence as well as melting were presented as a function of time. Results were validated by comparison with experimental observations in the literature covering relevant range of alloying materials and flow velocities. According to validations, simulations of real alloying materials using developed model can be done with good accuracy for industrial heats in argon stirred ladles.

Introduction

The knowledge on alloy melting and mixing in steel melt has grown during the last two decades revealing the great complexity of the process. That raises several problems in modeling of phenomena in alloying. These problems and phenomena have been investigated by many groups and investigators during the years, e.g. Fruehan, Szekely and Oeters [1-3]. The extensive overview of physical and mathematical modeling of gas stirred ladle systems has been published by Mazumdar and Guthrie [4]. Alloy addition into steel melt consists of melting and mixing stages. Melting contains two periods, namely the shell period and the melting of the particle core itself. Mixing plays an important part in homogenizing the steel. It also influences heat transfer and thus the life time of the solid shell. Melting and mixing of alloying additions is a multiphase process that is dependent on many factors. The alloying additive and its impurities itself, the temperature of the melt and the addition and the mixing methods are very significant when aiming for the optimal result.

The particle size and density of the additive is also important. Bigger particle causes a bigger heat sink in the steel melt surrounding it. The solid shell forming around the particle grows also thicker because of this larger heat difference. Hence, the melting of the shell formed takes a longer time. If the density of the alloy is significantly lower than the steel's density, the submersion time of the particles is not sufficient for the alloy to melt into the steel. In consequence, the added lump with solidified steel shell enters to the slag-metal interface where it then finally melts down.

Melting temperature of the additive is also important when selecting the particle size used. If the melting temperature of the additive is lower than the steel melting temperature, the core of the additive can be in molten state before the shell has disappeared. Bigger particles take a longer time to heat up to melting temperature and they might need preheating before adding to melt to ensure the desired result.

The shell forming around the surface of the particle added to the steel melt is a factor that presents many complications in modeling the melting of alloying additions. Because the shell formation is dependent on many process parameters and of the added particle itself, it is complicated to make a model that could give accurate information on the melting of the particle.

Mathematical modeling of alloy melting

In this study the focus of mathematical modeling is on behaviour of single alloy particle when it is in flowing liquid steel bath. When alloy addition enters the liquid steel, it causes a heat sink and severe local chilling of the steel in the nearby area. This leads to a shell of steel forming around the alloy fragment. The alloy particle inside the shell is pre-heated. If the alloy has a lower liquidus temperature than the solidification temperature of the surrounding steel, part of the particle can be molten before the steel shell is completely re-melted. An example of this is ferromanganese which has a liquidus temperature below that of the steel. In this case dissolution of the substance is not important. If the liquidus temperature of the alloy to be melted is higher than the temperature of the surrounding liquid, dissolution becomes important.

Mathematical model was done using commercial CFD software (Flow-3D from Flow Science Inc.) using its default RNG turbulence model. Interpretation of the simulation results was found out to be difficult. Thickness of solidified shell is easy to compute from the results when the steel is not flowing in simulations. However when steel flow is present in the simulation (as it is during ladle stirring), the iron shell does not grow equally over an alloy, but is thicker at the back (silent) side of the particle (Figure 1). This unevenness can lead to the situation where the iron shell has been disappeared everywhere but at the back of the particle. If the shell existence time in simulations is considered as the time when the iron shell breaks down for the first time, results of the simulations are comparable with the literature.

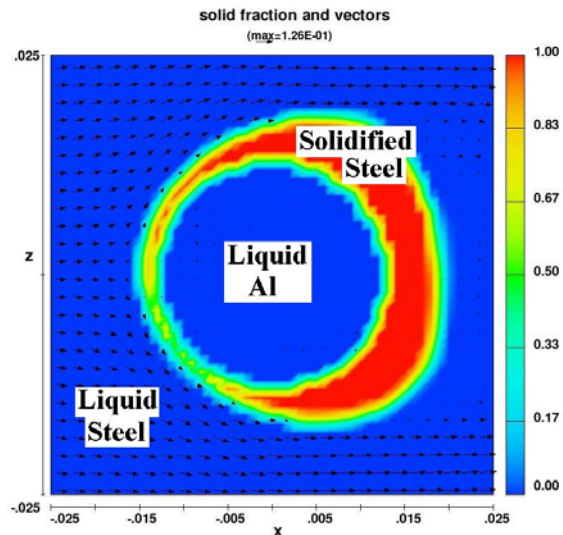


Figure 1: Example of shell unevenness in simulation; $v = 0.1$ m/s, $t = 4$ s (x and z axis in meters)

First validation case was with aluminium [5]. Steel temperature (both initial and incoming) was 1600°C and steel velocity was fixed at 0.4 m/s. Spherical aluminium particle (used material properties are listed in Table 1) with radius of 1 centimeter was fixed to its location in the center of calculation mesh. Initial temperature of the particle was 100°C . Because of clear challenges in post-processing of the simulations, which was also mentioned by Gardin et.al [5], validations were decided to carry out in both 2D and 3D. Unfortunately shell unevenness is even more challenging when the modelling geometry is 3 dimensional.

Comparison of results with 2D and 3D simulations

Simulation results showed same kind of behaviour as validation results, but accuracy was good only with certain velocity range. In 3D-simulations that velocity range was between 0.1 - 0.4 m/s and in 2D-simulations between 0.4 - 0.8 m/s (Figure 2). Because of relatively poor correlation some additional validations were decided to conduct.

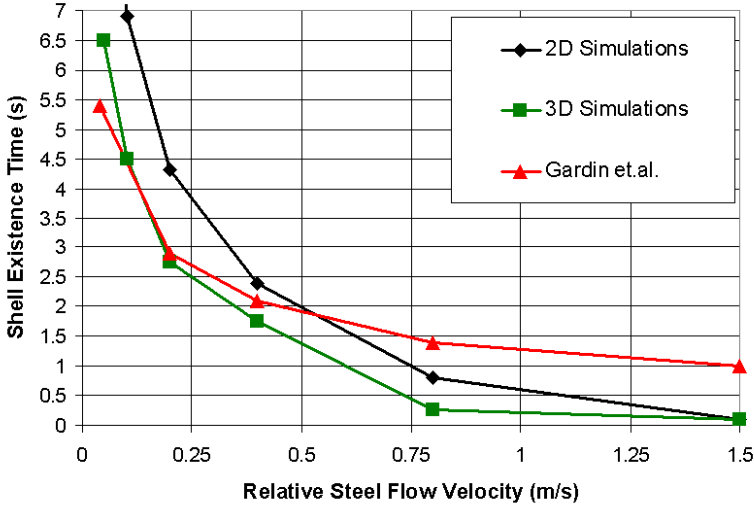


Figure 2: Difference in shell existence times with different relative steel flow velocities (pure aluminium particle with radius of 1 cm). Temperature 1600°C.

Because of unevenness of the growing shell and complexity of interpretation of 3D-simulation results, it makes difficult to find out e.g. real shell existence time from 3D-simulations. Also longer simulation times in 3D, made use of 2D simulations more preferable and therefore these additional validation were done only in 2D.

Validations using manganese and nickel particles

Zhang and Oeters [6] calculated shell development and alloy melting with different sized manganese (Mn) and nickel (Ni) particles (used material properties are given in Table 1). Main results were from calculations where steel flow velocity was 0.1 m/s. This gave good additional validation data, since with this velocity value case validation would be done outside of suggested good velocity range from the previous validations. Besides of that use of different sized particles (size range was from 1 to 4 cm) will also give us better understanding of mathematical model's accuracy.

Table 1: Material properties of aluminium, manganese, nickel and steel [5, 6]

Material	T_s (°C)	ΔH_s (kJ/kg)	λ (W/mK)	C_p (J/kgK)	ρ (kg/m ³)
Al	660	397	237	900	2700
Mn	1250	266.5	50	800	7290
Ni	1455	292.2	85.5	570	8910
Steel	1546	272	35	800	7000

In these simulations particles were also simplified as spheres. Initial temperature of particles was 25 °C and surrounding liquid steel temperature to be 1600 °C.

Simulations with manganese particles showed slightly different shell growth than what Zhang and Oeters calculations resulted. This might be result from differences between pure mathematical modelling, which Zhang and Oeters used, and CFD modelling, which was used in our simulations. In mathematical modelling e.g. steel shell forms uniformly around the particle and also melts uniformly away. In CFD-modelling, as already showed in Figure 1, steel flow forms anomalies to shell shape. In our simulations smaller manganese particles (radius of 1 cm and 2 cm) results were close to each others. Difference was only couple of seconds. However difference between results grows bigger when comparing results from larger particles. With 3 cm particle shell exists almost 10 seconds longer in Zhang and Oeters simulations than with our simulations and time difference is 20 seconds in 4 cm particle.

Even though same behaviour, as what was seen with manganese particles, can also be seen with nickel particles (Figure 3), accuracy in nickel particle simulations is much better. Difference in shell existence times with 1-3 cm particles is only couple of seconds, but in contrast to manganese particles, time difference is about the same even with largest (radius 4 cm) particle.

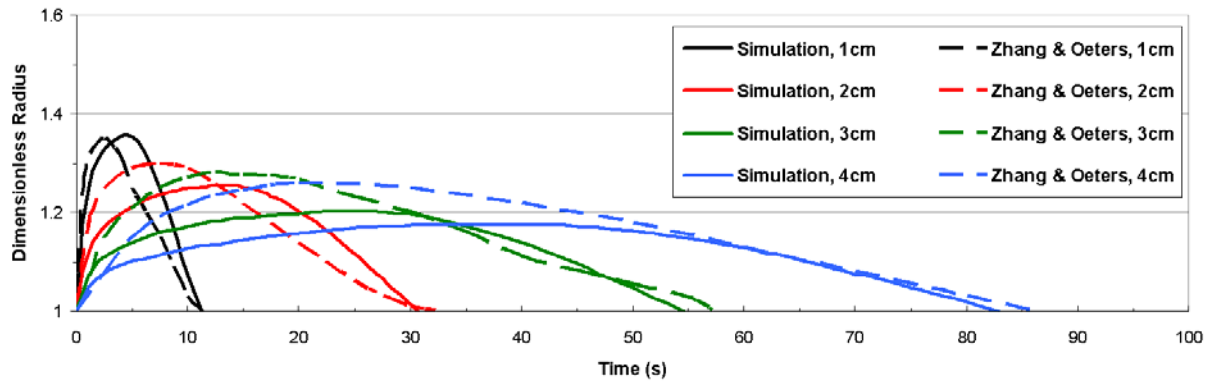


Figure 3: Shell existence time validations for nickel particles

Size of the alloy materials in real ladle process usually differs between 5 and 100 mm in diameter, which convert to radius of 0.25-5 cm (when simplified to sphere). Most of the alloy particles have radius smaller than 2 cm. Since validation with manganese and nickel particles gave very good accuracy with small particles (1-2 cm), it was decided that used model could be used to model also the real alloying addition materials.

Melting of alloying additions

The mathematical model was subsequently utilised to calculate the melting times of alloying additions as used in the real process with the aim to find the minimum stirring time for complete melting of the alloying additions and to help to develop adapted ladle stirring strategies. Some major alloying materials were selected for simulations. Selected alloying materials and their properties are presented in Table 2.

Table 2: Material properties of simulated alloying materials [6]

Alloying material	T_s (°C)	ΔH_s (kJ/kg)	λ (W/mK)	C_p (J/kgK)	ρ (kg/m ³)
FeSi	1316	1446.6	2.93	938	2800
FeMn	1266	207.5	8.368	911	7180
FeCr	1532	309	12.55	891	6900
SiMn	1215	493.8	4.184	844	6120

Again alloy particle is fixed to the one position and liquid steel has given mean velocity, which was selected to be 0.5 m/s. In gas-stirred ladle velocities at the top of the ladle are usually considered to be somewhere in between 0.5-1.0 m/s [7]. Many of the alloying materials, which were simulated, have smaller density than steel. This density difference between steel and alloy evokes lift force towards the surface. The magnitude of lift force varies with different particles. However, since comparison of the simulations is easier with a same fixed velocity for all cases, estimation for relative steel flow velocity was needed.

Effect of alloying material and particle size

Melting times differ quite much depending on the material and particle size. Aluminium is the only simulated alloy material which has very short dissolution time which is equal to the existence time of the solidified steel shell due to low melting point of aluminium. The difference in particle melting times (0.45s - 1.15s) is related to the size of Al-particles (6 mm to 12 mm). Faster melting of aluminium is mainly because of two reasons that make aluminium different from other simulated alloys. The first reason is that the melting point of aluminium is much lower than any other alloy in focus (T_s of Al is only 660 °C, when the next closest one is 1215 °C of SiMn). The second reason is the much higher value of thermal conductivity of aluminium. When other alloying materials have conductivity less than 15 W/mK, aluminium features a conductivity of almost 250 W/mK.

FeSi, which had second smallest difference in simulated particle sizes (from 20 mm to 100 mm), showed 27 second difference in shell existence times. However, because of material properties of FeSi, the total melting time (time needed for all alloy material to melt) varied between different particle sizes with over about 220 seconds. Differences observed in total melting time with SiMn and FeMn, which both had even larger particle size variation, were “only” 130s - 140s. This happened even though shell existence times were longer than with FeSi.

Largest difference between different particles was observed with FeCr. It took about 2 seconds to melt the steel shell with smallest particles (diameter 5mm), when it was with the largest particles (diameter 100 mm) almost 140 seconds. Total melting time of largest FeCr-particles could be over 330 seconds.

Differences between different alloying materials are more evident when comparing same sized particles of different alloy. With smallest particles (diameter less than 10 mm) melting times are

so short, that basically they have no differences. 40 mm and especially 100 mm particles give us better data for comparison (Figure 4). It is clear that both shell breaking and total melting times of FeCr-particles are longest. What makes FeCr so different from other simulated materials, is its very high melting point. FeCr has melting point of 1532 °C which is over 200 degrees centigrade higher than the next highest one (FeSi 1316 °C).

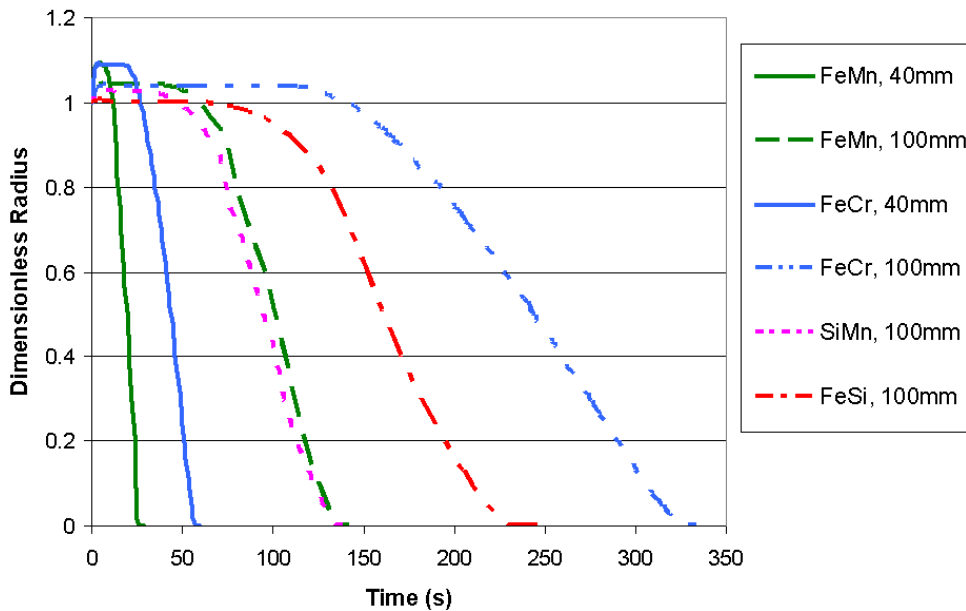


Figure 4: Melting time comparison of large alloy particles (diameters 40-100 mm)

From rest of the alloying materials, FeMn and SiMn behaved almost the same way, only slight differences appeared in shell breaking times. They shared almost same melting point (FeMn 1266°C and SiMn 1215 °C) which is the most important reason for their similar melting behaviour. Differences in conductivities explain slight differences in shell existence times between these two alloys. Even though conductivities have almost same numerical values, FeMn's values are double of what SiMn has and so steel shell has better ground to build. However, SiMn has much higher latent heat, which evens situation, as melting of SiMn will take longer time compared with FeMn.

As it was mentioned earlier peculiar melting behaviour of FeSi is caused of very high latent heat value. Melting of FeSi will require more energy than with other alloys and even though shell existence time is in comparison significantly shorter, total melting time of FeSi is the second longest after FeCr.

When taking validation results into account, melting times of largest particles can be even longer. Also a particular problem appears with especially large and dense particles if they manage to descent close to the ladle bottom the melting times can grow even longer than in the present study. This is because velocities are more likely to be slower than in the vicinity of the upward directed gas flow (plume). According to these simulation results it is clear, that certain planning is useful in alloy addition.

Effect of steel velocity on melting times

The objective of the calculations was to identify minimum steel flow velocities and therefore stirring gas flow rates (steel flow is induced by stirring) for optimum melting of the alloying additions.

Aluminium differs from other alloying materials especially with much lower melting temperature and also with smaller variation of particle size. Melting times for both 6mm and 12mm diameter are less than 5 seconds, which would indicate that melting of Al does not demand any particular changes in stirring practice

Simulated ferrosilicon (FeSi) particles had diameters of 20 mm and 100 mm. Unlike with aluminium, particle size difference with FeSi and therefore also melting time difference is much larger. Maximum melting time with smaller FeSi-particle is about 50 seconds when with larger particle it is almost five times longer. However velocity dependence curves with both particle sizes are close to each other: melting times are first shortening rapidly when moving from very low velocities to higher and then reaching some kind of limit value around 0.5-0.6 m/s. So unlike with Al, with FeSi it is possible to find optimum velocities for melting. When velocities are lower than 0.25 m/s, melting times start to rise quickly and on the other hand, melting times do not shorten in practice at all, when velocities are higher than 0.55 m/s. Therefore, the optimum velocities for FeSi melting are between 0.25 and 0.55 m/s.

The size of FeMn additions used in steelmaking varies from 5 to 100 millimeters and therefore also maximum melting times vary from less than 10 seconds to 400 seconds. Also minimum melting times have large difference, from less than a second to 120 seconds. Like FeSi it is also clear to see velocity dependence of the melting times. When using higher steel flow velocities, melting time do not change almost at all when velocity is over 0.5 m/s. With lower velocities, high increase in melting times is visible after 0.2-0.3 m/s. The optimum velocity range is located between 0.25 and 0.5 m/s.

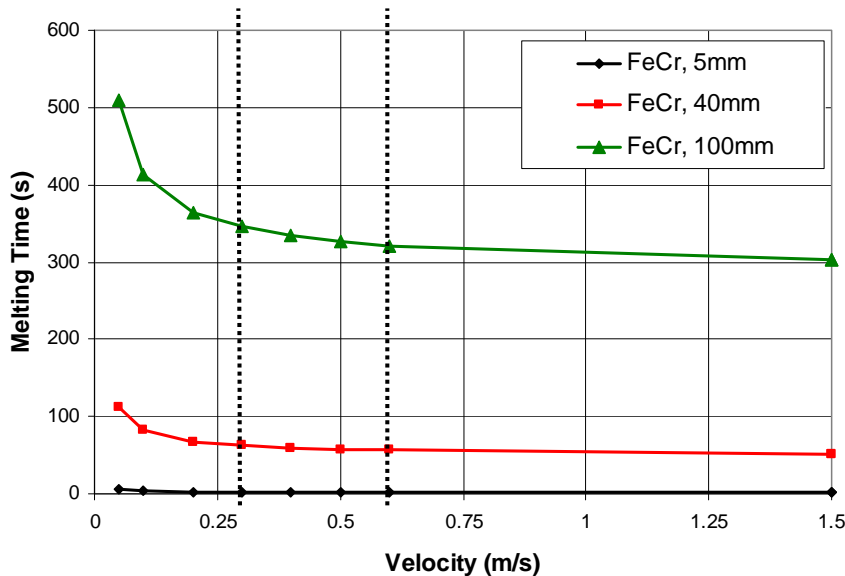


Figure 5: Melting times of 5 mm, 40 mm and 100 mm FeCr-particles

Ferrochromium (FeCr) had longest melting times of all simulated materials. With largest particle (diameter 100 mm), the minimum melting time was slightly over 300 seconds and the maximum melting time was reaching 500 seconds (Figure 5). The melting time vs. velocity curves are as clear as with FeSi and FeMn earlier, showing an optimum velocity range between 0.3 and 0.6 m/s.

Melting times of silicomanganese (SiMn) particles reach equilibrium with slightly lower velocities compared to other alloying materials. Melting times do not change significantly with velocities higher than 0.4 m/s.

The steel flow velocities to reach optimum melting times of alloying additions are summarised in Table 3. Appropriate melting of all types of alloying additions can be reached using steel flow velocities as low as 0.3 m/s. Velocity of liquid steel in an industrial ladle generally will exceed a threshold velocity of 0.3 m/s. Studies have shown that the velocity can be over 0.7 m/s even with a low stirring gas flow rates (20 STP m³/h or less in 170 ton ladle) [7]. Under these conditions, the resulting mixing time of the alloying addition that takes longest to melt (100 mm FeCr) is approximately 350 s. Therefore, even when stirring with reduced stirring intensity, six minutes of stirring leads to complete melting of all alloying additions. With very strong stirring (e.g. 40 m³/h or more in 170-t ladle), this melting time could only be reduced by one minute.

Table 3: Steel flow velocities for optimum melting of alloying additions

Alloying addition	Minimum steel flow velocity (m/s)	Maximum steel flow velocity (m/s)
FeSi	0.25	0.55
FeMn	0.25	0.50
FeCr	0.30	0.60
SiMn	0.25	0.40

Conclusions

A simple practical mathematical model was developed to describe the behaviour of different alloys when added into ladle. The model was made using commercial CFD software and it focused on the behaviour of the single alloy particle. Simulation of the shell formation procedure is divided into two stages: in the first stage a cold alloy lump is introduced into the liquid steel; solid shell starts to form, it grows to a maximum thickness and then starts to melt and finally disappears. In the second stage the lump itself melts (if not yet molten) and is mixed into the bulk steel in the ladle. Model testing was done by comparing the results with multiple literature cases which covered suitable range of different flow velocities and alloying materials. According extensive validations, simulations of the real alloying materials using developed model can be done with good accuracy. The model was used to study the dependence between total melting time of industrial alloying material particles of different sizes and steel flow velocity, which is essential for optimisation of the ladle stirring practice.

Acknowledgements

This research was done within the project “Improvement of ladle stirring to minimise slag emulsification and reoxidation during alloying and rinsing” which was carried out with a financial grant of the Research Programme of the Research Fund for Coal and Steel (RFSR-CT-2007-00009).

List of symbols

C_p	Heat capacity (J/kg*K)
λ	Heat conductivity (W/m*K)
ρ	Density (kg/m ³)
σ	Interfacial tension (mN/m)
ΔH_s	Latent heat (kJ/kg)
T_s	Solidus temperature (°C)
v	Velocity (m/s)
x, y, z	Coordinate axes

References

- [1] R.J. Fruehan, “Ladle metallurgy principles and practices”, Iron and Steel Society, 1985, ISBN 0-932897-01-0
- [2] J. Szekely, G. Carlsson, and L. Helle, “Ladle Metallurgy”, Springer-Verlag, New York, 1989, ISBN 0-387-96798-2
- [3] F. Oeters, “Metallurgy of Steelmaking”, Stahleisen, 1994, ISBN 3-514-00465-X
- [4] D. Mazumdar and R.I.L. Guthrie, ”The Physical and Mathematical Modelling of Gas Stirred Ladle Systems”, ISIJ International, Vol.35 (1995), No. 1, pp.1-20
- [5] P. Gardin, J.-F. Domgin, M. Simonnet, and J. Lehmann, “Modeling of inclusion evolution in a steel ladle or in RH degasser”, Revue de Métallurgie, No. 2 (2008), pp. 84-91
- [6] L. Zhang and F. Oeters, “Melting and mixing of alloying agents in steel melts – Methods of mathematical modeling”, Stahleisen, 1999, ISBN 3-514-00637-7
- [7] P. Valentin, C. Bruch, Y. Kyrylenko, H. Köchner, and C. Dannert, “Influence of the Stirring Gas in a 170-t Ladle on Mixing Phenomena – Formation and On-line Control of Open-Eye at an Industrial LD Steel Plant”, Steel Research International, Vol. 80 (2009), No.8, pp. 552-558